

# Energy-Spectral Efficiency Trade-Off in Underlying Mobile D2D Communications: An Economic Efficiency Perspective

Rui Zhang<sup>1</sup>, Yongzhao Li, *Senior Member, IEEE*, Cheng-Xiang Wang<sup>2</sup>, *Fellow, IEEE*,  
Yuhan Ruan<sup>1</sup>, Yu Fu, and Hailin Zhang<sup>3</sup>, *Member, IEEE*

**Abstract**—With a great potential to support multitudinous services and applications, mobile device-to-device (D2D) communications are conceived as a candidate paradigm for the future intelligent transportation systems and mobile Internet. To optimize the performance of underlying mobile D2D communication systems with mutual interference caused by resource reuse, we propose two scenario-related power allocation schemes and investigate the energy efficiency (EE) and spectral efficiency (SE) trade-off. A 3-D vehicle-to-vehicle channel model is adopted to characterize propagation characteristics in realistic vehicular environments. We observe that a small degradation in EE around its peak value can significantly increase the SE for high vehicular traffic density (VTD) scenarios, while a marginal degradation in SE results in a considerable gain in EE for low VTD scenarios. Therefore, we maximize the SE subject to EE requirement in high VTD scenarios and maximize EE subject to SE requirement in low VTD scenarios. Moreover, to provide comprehensive understanding and further facilitate the practicality of EE-SE trade-off, economic efficiency (ECE) is employed as a general evaluation criterion to assess the efficacy of tradeoff. Finally, extensive simulations are provided to reveal the tradeoff quantitatively and demonstrate the viability that ECE can serve as a general metric for EE-SE trade-off in vehicular environments under different communication conditions.

**Index Terms**—Mobile device-to-device communications, power allocation, energy efficiency, spectral efficiency, economic efficiency.

Manuscript received May 24, 2017; revised September 18, 2017 and December 27, 2017; accepted March 15, 2018. Date of publication April 10, 2018; date of current version July 10, 2018. This work was supported in part by the National Key Research and Development Program of China under Grant 2016YF-B1200202, in part by the National Natural Science Foundation of China under Grant 61771365, in part by the Natural Science Foundation of Shaanxi Province under Grant 2017JZ022, in part by the 111 Project under Grant B08038, in part by the EU H2020 RISE TESTBED Project under Grant 734325, in part by the EU FP7 QUICK Project under Grant PIRSES-GA-2013-612652, and in part by the EPSRC TOUCAN Project under Grant EP/L020009/1. The associate editor coordinating the review of this paper and approving it for publication was W. Saad. (*Corresponding author: Yongzhao Li.*)

R. Zhang, Y. Li, Y. Ruan, and H. Zhang are with the State Key Laboratory of Integrated Services Networks, Xidian University, Xi'an 710071, China (e-mail: rui\_zhang\_xd@163.com; zhli@xidian.edu.cn; ryh911228@163.com; hlzhang@xidian.edu.cn).

C.-X. Wang and Y. Fu are with the Institute of Sensors, Signals and Systems, School of Engineering and Physical Sciences, Heriot-Watt University, Edinburgh EH14 4AS, U.K. (e-mail: cheng-xiang.wang@hw.ac.uk; y.fu@hw.ac.uk).

Color versions of one or more of the figures in this paper are available online at <http://ieeexplore.ieee.org>.

Digital Object Identifier 10.1109/TWC.2018.2822284

## I. INTRODUCTION

ENABLING users in proximity to directly communicate with each other, Device-to-Device (D2D) communications have a great potential to reduce transmission power and increase transmission data rates [1], [2]. Meanwhile, coexisting with conventional cellular networks in an underlay manner, D2D communications can also significantly increase spectrum utilization [3]. Therefore, D2D communications have emerged as one of the most promising technologies for cellular networks to increase spectral efficiency (SE) and energy efficiency (EE), both of which are crucial design requirements for the future fifth generation (5G) wireless networks [4]. However, the mutual interference caused by resource reuse is still a major obstacle to integrate D2D communications into cellular networks. It not only hinders the performance of D2D communications but also degrades the quality of cellular communications [5].

To achieve the envisioned advantages of D2D communications, interference management and resource allocation schemes have received enormous attention. In this regard, the authors in [6] presented an interference limited area control scheme to increase the capacities of both cellular and D2D communication systems, where the interference received at D2D users remained below a predetermined threshold. Taking the signal-to-interference-plus-noise ratio (SINR) requirements for both D2D and cellular users into account, the authors in [7] proposed a resource allocation scheme to maximize the overall throughput. Meanwhile, an iterative Hungarian method was proposed in [8] to maximize the network throughput with joint relay selection and resource allocation. The above studies concentrated on optimizing system performance from the perspective of capacity. Besides, energy efficient resource allocation strategies for underlying D2D communications have also attracted tremendous attentions to reduce the excessive energy consumption in 5G wireless networks. A contract-based pricing mechanism was proposed in [9] to encourage users to conduct coordination with others to reduce energy consumption. To maximize the EE of cellular and D2D users, the authors in [10] and [11] investigated a joint mode selection and power control scheme and a channel quality indication based resource reuse scheme, respectively. The authors in [12] and [13] presented a joint resource allocation and power

control scheme to maximize the EE of D2D communications. The authors in [14] focused on minimizing the power consumption, assuming that idle users could act as relays to enhance the communication between cellular users and the base station (BS). Similarly, the authors in [15] proposed a mobile association scheme to maximize the EE of relay aided D2D communications while guaranteeing the minimum rate requirement of cellular users. Besides, the authors in [16] investigated an optimal power allocation scheme for multiple D2D pairs, which share the same resource to improve the utilization of the wireless spectrum.

Recently, D2D communication were also conceived as a candidate paradigm to provide ultra-reliable and low latency services or high data rate required applications for drivers and passengers in future intelligent transportation systems and mobile Internet [17], [18]. However, the introduction of mobile users in vehicular environments poses new challenges, especially in terms of radio resource allocation [19]. In this regard, the authors in [20] proposed reuse channel selection and power control schemes to optimize the data rate. Considering both the delay and reliability requirements of mobile D2D users, the authors in [21] and [22] proposed resource management schemes to maximize the capacity of cellular users under different resource reuse strategies. Moreover, a location dependent resource allocation scheme was introduced in [23] to deal with resource reservation problems in terms of throughput and delay.

It is noticeable that the aforementioned studies only considered simplified distance model [23] or large scale fading model [19]–[22]. However, in a realistic vehicular environment, the high mobility of D2D users and/or the vehicular traffic density (VTD)<sup>1</sup> may have a significant impact on the propagation characteristics of wireless channels [24]–[26]. An inaccurate channel model may result in inaccurate system performance evaluations in terms of capacity, throughput, transmit power consumption, and so on. To the best of our knowledge, the performance of underlying mobile D2D communications under reasonable and applicable channel models has not been well investigated. Moreover, the authors in [19]–[23] only concentrated on optimizing the performance of mobile D2D communications from the perspective of capacity, while the consideration of both SE and EE is significant in mobile D2D communications [4], [27]. For conventional D2D communications, the authors in [28] studied the trade-off between EE and SE, while the interference constraint imposed by cellular communications was not considered. For underlying mobile D2D communications, where the propagation characteristics of vehicular environments have great impacts on system performance, the research on trade-off between EE and SE is still missing. Moreover, how to quantitatively evaluate the rationality and efficacy of the trade-off has not been well investigated, which is an increasingly important area nowadays [29].

To fill these gaps, we investigate the trade-off between EE and SE of underlying mobile D2D communications and examine how the characteristics of vehicular environments affect the EE and SE trade-off, which governs the practical implementation of power allocation schemes to optimize network performance. We can highlight the novelties and contributions of this paper as follows:

- 1) **The EE-SE trade-off of mobile D2D communications undelaying cellular networks is investigated for the first time.** Due to the fact that maximizing EE and maximizing SE are conflicting objectives, the trade-off between EE and SE is a critical issue in the design of wireless communication systems [29]. Taking the mutual interference between D2D and cellular communications into account, we investigate the trade-off between EE and SE in an underlying mobile D2D communications scenario, where a three-dimensional (3D) vehicle-to-vehicle (V2V) channel model is adopted to characterize the mobility of D2D users and the VTD in a realistic vehicular environment.
- 2) **Two scenario-related power allocation schemes that adapt the preference of EE or SE in different vehicular environments are proposed for the EE-SE trade-off.** We observe that a small degradation in EE around its peak value can significantly increase the SE for high VTD scenarios, while a marginal degradation in SE results in a considerable gain in EE for low VTD scenarios. Therefore, we formulate power allocation schemes as EE optimization problem for low VTD scenarios and SE optimization problem for high VTD scenarios, which is different from current studies that blindly maximizes EE or SE, e.g., [28]. Moreover, we obtain optimal solutions expressed as functions of EE threshold or SE threshold, which are decisive parameters in terms of the trade-off between EE and SE.
- 3) **Economic efficiency (ECE) is employed as an evaluation metric for the efficacy of EE-SE trade-off from the perspective of benefit and cost.** For the EE and SE trade-off, to what extent we should sacrifice either EE or SE, i.e., how to determine the value of SE or EE thresholds, is still an open issue in terms of the viability of the EE-SE trade-off. To provide comprehensive understanding and to further facilitate the practicality of EE and SE trade-off, we employ ECE, which measures the profitability (in monetary unit per second) of communication systems, as a general metric to assess the efficacy of trade-off.

The remainder of the paper is organized as follows. Section II introduces the system model. Section III investigates the EE and SE trade-off in different VTD scenarios. In Section IV, the ECE is introduced as a general metric to evaluate the rationality of EE and SE trade-off. Simulations and discussions are given in Section V. Finally, conclusions are given in Section VI.

## II. SYSTEM MODEL

In this paper, we take a D2D communication unit, consisting of one BS, one D2D pair, and one cellular user (CU), as an

<sup>1</sup>Here, VTD is the number of vehicles around the transmitter and receiver. In vehicular communications, vehicles acting as obstacles can notably obstruct the line-of-sight propagation.

example to investigate EE-SE trade-off and the associated power allocation in mobile D2D communications underlying cellular networks.<sup>2</sup> In one D2D pair, the source user (SU) will communicate with the destination user (DU) sharing the same radio resources as the CU used in uplink transmissions, where the DU will be interfered by the CU and the BS will also suffer from the interference from the SU. In addition, we assume each node is equipped with a single antenna. We denote  $h_{sd}$ ,  $h_{sb}$ , and  $h_{cd}$  as the channel coefficients of SU→DU, SU→BS, and CU→DU links, respectively. By denoting  $m \triangleq \{sd, sb, cd\}$ , we have  $|h_m|^2 = |g_m|^2 PL(d_m)$  with  $g_m$  as the small-scale fading gain,  $d_m$  as the distance, and  $PL(d_m)$  as the pathloss.<sup>3</sup> In the following, we first introduce the adopted 3D V2V channel model, which has various unique channel parameters. These parameters determine propagation properties of different VTD scenarios, which enlighten our work in this paper.

### A. Channel Model

Since both the SU and DU can have high mobility, the traditional channel model where either the transmitter or the receiver is assumed motionless is no longer applicable to mobile D2D communications [25]. On the other hand, surrounding vehicles acting as obstacles can greatly affect the signal propagation in vehicular environment [24]. To accurately capture the effect of the mobility of D2D users and moving vehicles on the channel characteristics, all involved links are modeled as the 3D V2V channel model proposed in [30], which is applicable to scenarios where users with various velocities as long as they are in a vehicular environment.

In this model, the radio propagation environment is characterized by 3D effective scattering with line-of-sight (LoS) and non-LoS (NLoS) components between the SU and the DU. Specifically, the NLoS components can be further classified as single bounced (SB) rays representing signals reflected only once during the propagation process and double bounced (DB) rays representing signals reflected more than once. Noteworthily, different from physical scatterers, an effective scatterer may include several physical scatterers which are unresolvable in delay and angle domains. Moreover, this channel model utilizes a two-sphere model to mimic the moving scatterers, such as other vehicles, and an elliptic-cylinder model to depict the stationary roadside environments, such as buildings and trees. Around the transmitter, there are  $N_1$  effective scatterers and the  $n_1$ th ( $n_1 = 1, \dots, N_1$ ) effective scatterer is denoted by  $s^{(n_1)}$ . Around the receiver,

there are  $N_2$  effective scatterers and the  $n_2$ th ( $n_2 = 1, \dots, N_2$ ) effective scatterer is denoted by  $s^{(n_2)}$ . Similarly, there are  $N_3$  effective scatterers in the elliptic-cylinder model and the  $n_3$ th ( $n_3 = 1, \dots, N_3$ ) effective scatterer is denoted by  $s^{(n_3)}$ . The geometry of the single- and double-bounced two-sphere model and other related details can be found in [30].

According to [30], the channel coefficient  $g(t)$  at the carrier frequency  $f$  is a superposition of the three types of components, which can be expressed as

$$g(t) = g_{\text{LoS}}(t) + \sum_{i=1}^I g_{\text{SB}_i}(t) + g_{\text{DB}}(t) \quad (1)$$

where  $g_{\text{LoS}}(t)$ ,  $g_{\text{SB}_i}(t)$ , and  $g_{\text{DB}}(t)$  are the LoS component, SB components, and DB components, respectively. In this model,  $I = 3$ , which means that there are three kinds of subcomponents for SB rays, i.e., SB<sub>1</sub> from the transmitter sphere, SB<sub>2</sub> from the receiver sphere, and SB<sub>3</sub> from the elliptic-cylinder. According to [30], we have

$$g_{\text{LoS}}(t) = \sqrt{\frac{K}{K+1}} e^{-j2\pi f \tau} e^{j2\pi f_s t \cos(\alpha_s^{\text{LoS}} - \lambda_s) \cos \beta_s^{\text{LoS}}} \times e^{j2\pi f_d t \cos(\alpha_d^{\text{LoS}} - \lambda_d) \cos \beta_d^{\text{LoS}}} \quad (2)$$

$$g_{\text{SB}_i}(t) = \sqrt{\frac{\eta_{\text{SB}_i}}{K+1}} \lim_{N_i \rightarrow \infty} \sum_{n_i=1}^{N_i} \frac{1}{\sqrt{N_i}} e^{j(\xi_{n_i} - 2\pi f \tau_{n_i})} \times e^{j2\pi f_s t \cos(\alpha_s^{(n_i)} - \lambda_s) \cos \beta_s^{(n_i)}} \times e^{j2\pi f_d t \cos(\alpha_d^{(n_i)} - \lambda_d) \cos \beta_d^{(n_i)}} \quad (3)$$

$$g_{\text{DB}}(t) = \sqrt{\frac{\eta_{\text{DB}}}{K+1}} \lim_{N_1, N_2 \rightarrow \infty} \sum_{n_1, n_2=1}^{N_1, N_2} \frac{1}{\sqrt{N_1, N_2}} \times e^{j(\xi_{n_1, n_2} - 2\pi f \tau_{n_1, n_2})} \times e^{j2\pi f_s t \cos(\alpha_s^{(n_1)} - \lambda_s) \cos \beta_s^{(n_1)}} \times e^{j2\pi f_d t \cos(\alpha_d^{(n_2)} - \lambda_d) \cos \beta_d^{(n_2)}} \quad (4)$$

where  $\alpha_s^{\text{LoS}} \approx \beta_s^{\text{LoS}} \approx \beta_d^{\text{LoS}} \approx 0$  and  $\alpha_d^{\text{LoS}} \approx \pi$  with  $\alpha_s^{\text{LoS}}$ ,  $\alpha_d^{\text{LoS}}$ ,  $\beta_s^{\text{LoS}}$ , and  $\beta_d^{\text{LoS}}$  denoting azimuth angles of departure (AoD), azimuth angles of arrival (AoA), elevation AoD, and elevation AoA of the line-of-sight (LoS) component, respectively. Here,  $\alpha_{s/d}^{(n_i)}$  and  $\beta_{s/d}^{(n_i)}$  are the azimuth AoD/azimuth AoA and elevation AoD/elevation AoA of the waves traveling from the effective scatterers  $s^{(n_i)}$ , respectively. Path delays for paths SU → DU, SU →  $s^{(n_i)}$  → DU, and SU →  $s^{(n_1)}$  →  $s^{(n_2)}$  → DU are defined as  $\tau$ ,  $\tau_{n_i}$ , and  $\tau_{n_1, n_2}$ , respectively. We have  $K$  designates the Rician factor, indicating the power ratio of the LoS component to NLoS components. The SU and DU are assumed to be moving at the speed of  $\nu_{s/d}$  in the direction angle of  $\lambda_{s/d}$ , and  $f_s$  and  $f_d$  are the Doppler frequencies with respect to the SU and the DU, respectively. Parameters  $\eta_{\text{SB}_i}$  and  $\eta_{\text{DB}}$  specify the amount of power that SB and DB rays contribute to the total scattered power  $1/(K+1)$ , which satisfy  $\sum_{i=1}^I \eta_{\text{SB}_i} + \eta_{\text{DB}} = 1$ . Phases  $\xi_{n_i}$  and  $\xi_{n_1, n_2}$  are assumed to be independent and identically distributed random variables with uniform distributions over  $[-\pi, \pi)$ .

<sup>2</sup>Similar to [12] and [21], we assume that the resource of one CU can only be shared by one D2D pair. In this case, the 2-dimensional joint resource allocation and power control optimization problem can be transformed into two separate optimization problems. Power control schemes proposed for a single D2D pair and a single CU systems can be incorporated into resource management schemes and easily extended to multi-user systems. In this paper, we assume that resource allocation have been accomplished and the relevant methods can refer to [11].

<sup>3</sup>Similar to [31], we assume that these channels are quasi-static and the SU can obtain all the instantaneous channel state information, which can be obtained by adopting the sparsity structure based channel estimation approach proposed in [32].

According to [30, eq. (5)], the the probability density function of  $|g|^2$  can be calculated as

$$f_{|g|^2}(x) = (1+K)e^{-K}e^{-(1+K)x}I_0\left(2\sqrt{K(1+K)}x\right) \quad (5)$$

where  $I_0$  is the zero-order modified Bessel function of the first kind.

### B. Introduction of High VTD and Low VTD Scenarios

According to propagation characteristics in vehicular environments, various vehicular communication scenarios are often distinguished in the literature, e.g., highways, rural roads, and urban streets [31]. These practical scenarios can be abstracted to two typical scenarios, i.e., high VTD and low VTD scenarios. The distinctions between high and low VTD scenarios are summarized as follows<sup>4</sup>:

- 1) Different numbers of vehicles: High VTD represents urban areas with dozens of vehicles per square kilometer; while low VTD accounts for highway scenarios with less ten vehicles per square kilometer [26], [30].
- 2) Different Ricean factors  $K$ : For high VTD scenarios,  $K$  is around 1, indicating a severe multipath fading environment. For low VTD scenarios,  $K$  is around ten times or more than that in high VTD scenarios [30], [31].
- 3) Different energy-related parameters: Parameters  $\eta_{SB_i}$  and  $\eta_{DB}$  specify the amounts of power that the SB and DB rays contribute to the total scattered power, which satisfy  $\sum_{i=1}^I \eta_{SB_i} + \eta_{DB} = 1$ . For low VTD scenarios, the received scattered power is mainly from waves reflected by the stationary roadside environments. This indicates that  $\eta_{SB_3} > \max(\eta_{SB_1}, \eta_{SB_2}) > \eta_{DB}$  [30]. For high VTD scenarios, due to dense moving vehicles, the DB rays bear more energy than SB rays, i.e.,  $\eta_{DB} > \max(\eta_{SB_1}, \eta_{SB_2}, \eta_{SB_3})$  [30].
- 4) Different environment-related parameters: Environment-related parameters control the concentration of the distribution relative to the mean direction of scatterers [30]. Here,  $k^1$ ,  $k^2$ , and  $k^3$  are parameters at the sphere model of the transmitter, the sphere model of the receiver, and the elliptic-cylinder model, respectively. Normally,  $k^1$  and  $k^2$  in high VTD scenarios are smaller than that in low VTD. As the scatterers reflected from static roadsides are homogeneous, the values of  $k^3$  are the same in high VTD and low VTD [30].

### C. Power Consumption Model

Considering that the transmit power is reduced while the circuit power starts to dominate in short-distance communication, we consider non-zero circuit power consumption model in this paper. The power consumption in a mobile intelligent equipment usually comes from three parts: radio-frequency power, circuit power, and static power [33], [34]. For a required transmission power  $P_D$ , the power consumption of a practical power amplifier can be given by  $\varepsilon P_D$ , where  $1/\varepsilon \in (0, 1]$  denotes the drain efficiency of the power amplifier.

<sup>4</sup>Specific values of relevant channel parameters in the 3D V2V channel model can be found in Table 2 in Sec. V.

Circuit power  $P_0^C$  considers the power consumed by radio-frequency circuits (excluding the radio-frequency amplifier) and baseband processing circuits. Moreover, static power  $P_0^S$  concerns fixed power consumption incurred by equipment for other purposes rather than for data transmission. Under the given power consumption model, the total expenditure power for single user can be expressed as

$$P = \varepsilon P_D + P_0^C + P_0^S. \quad (6)$$

Since the circuits and static power consumption are usually independent of data rate and regarded as a constant for single mobile user, for notation simplicity, we use  $P = \varepsilon P_D + P_0$  in the following sections, where  $P_0 = P_0^C + P_0^S$ .

## III. EE AND SE TRADE-OFF IN UNDERLAYING MOBILE D2D COMMUNICATIONS

In this section, we investigate the trade-off between EE and SE from the perspective of power allocation with the 3D V2V channel model. Firstly, we introduce the definition of EE and SE based on the given power consumption model. We observe that a small degradation in EE around its peak value can significantly increase the SE for high VTD scenarios, while a marginal degradation in SE results in a considerable gain in EE for low VTD scenarios. Therefore, we contrastively formulate the power allocation schemes as two different optimization problems for different VTD scenarios. Specifically, we maximize the SE with minimum EE threshold in high VTD scenarios and maximize the EE with minimum SE threshold in low VTD scenarios, while guaranteeing the interference constraint imposed by cellular communications. Moreover, we derive the optimal solutions of transmission power in both high and low VTD scenarios, which are the expressions of SE threshold or EE threshold.

### A. Spectral Efficiency and Energy Efficiency Analysis in Different VTD Scenarios

As illustrated in [24] and [25], the VTD has a great impact on all channel statistical properties, which eventually affect the performance of EE and SE. Therefore, to facilitate the applicability and practicability of resource management, we should design the power allocation scheme according to the propagation characteristics of vehicular environment. In order to investigate the EE and SE performance in an underlaying mobile D2D communication scenario, we first introduce the definition of EE and SE.

Instantaneous EE ( $\Phi_{EE}$ , in bits/Hz/Joule) is defined as the ratio of the instantaneous SE ( $\Phi_{SE}$ , in bits/s/Hz) to the total power consumption ( $P$ , in Watt), which can be expressed as

$$\Phi_{EE} = \frac{\Phi_{SE}}{P} \quad (7)$$

where  $P = \varepsilon P_D + P_0$  with  $P_D$  as the transmission power of the SU. For a given system bandwidth  $W$ , the SE is written as

$$\Phi_{SE} = \frac{C}{W} = \log_2(1 + \gamma) \quad (8)$$

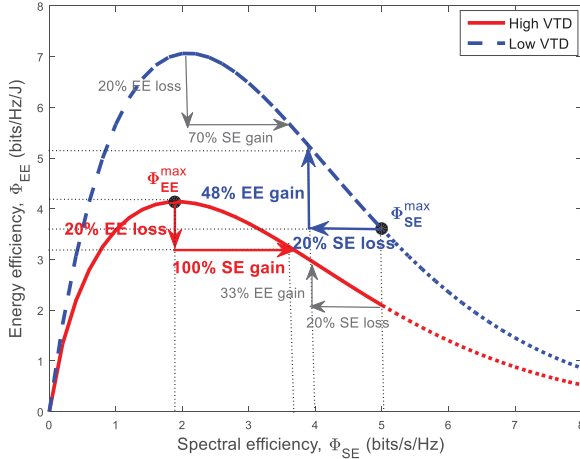


Fig. 1. EE versus SE in high VTD and low VTD scenarios ( $d_{sd} = 300$  m,  $P_0 = 100$  mW,  $I_{th} = -70$  dBm,  $P_C = 23$  dBm,  $v = 5$  m/s, and  $P_{max} = \infty$ ).

TABLE I  
EE/SE GAINS IN HIGH AND LOW VTD SCENARIOS

20% SE loss	high VTD	low VTD
EE gain	33%	<b>48%</b>
20% EE loss	high VTD	low VTD
SE gain	<b>100%</b>	70%

with  $C$  as the instantaneous capacity and  $\gamma$  as the received SINR of DU. We have

$$\gamma = \frac{P_D |h_{sd}|^2}{N_0 + P_C |h_{cd}|^2} \quad (9)$$

where  $N_0$  is the noise power of D2D receiver and  $P_C$  is the transmission power of the CU.

To explicitly reveal the EE-SE performance in different VTD scenarios, we plotted Fig. 1, from which the EE gain and SE gain in both high VTD and low VTD scenarios can be clearly observed. Here,  $I_{th}$  is the interference threshold of the BS,  $P_{max}$  is maximum transmit power of the SU, and  $v$  is the velocity of D2D users. The velocities of the BS and CU are assumed to be zero and the SU and the DU are moving toward each other with the same velocity. It is worth noting that the value of  $P_{max}$  only affects the maximum achievable EE and SE, rather than their relationship of trade-off. To give a holistic view of EE-SE performance in Fig. 1, we set  $P_{max}$  as infinity to include the achievable EE and SE as much as possible. As shown, the EE increases at the beginning and decreases afterwards in both scenarios. For low VTD scenarios, the slope of the curve is sharp at high values of SE, which reveals that a marginal degradation in SE results in a considerable gain in EE. While for high VTD scenarios, the slope of the curve is small around the maximum EE value, implying that a small degradation in EE around its peak value results in a significant gain in SE. From Fig. 1, the EE/SE gain in low VTD and high VTD scenarios can be summarized as in Table I.

It is worth noting that the objective of EE-SE trade-off is to investigate how to balance the EE and SE, i.e., sacrificing

EE or SE to improve the performance of the other one. In this case, it is expected that with the same loss of EE (SE), the SE (EE) increases as much as possible. It is obvious that with the same SE loss, low VTD scenarios can achieve higher EE gain. With the same EE loss, high VTD scenarios can achieve higher SE gain.

These observations illustrate the important impact of VTD on EE-SE performance in underlying mobile D2D communications and enlighten our work in the following, based on which we contrastively formulate two different optimization problems for low VTD and high VTD scenarios with the interference constraint imposed by cellular communications. Specifically, considering the objective of the EE-SE trade-off, the SE of mobile D2D users is maximized in high VTD scenarios and the EE of mobile D2D users is maximized in low VTD scenarios. For engineering application, one can distinguish these two scenarios based on practical communication environments. For example, we refer to the method proposed for low VTD when vehicular users are on the rural roads.

### B. Power Allocation in High VTD Scenarios

For high VTD scenarios, we propose to maximize the SE at the expense of EE, while the minimum EE is guaranteed and the interference from the SU to BS remains a tolerable level. By denoting  $\Gamma_{EE}$  as the EE threshold, the optimization problem can be formulated as

$$\begin{aligned} & \underset{P_D(h_{sd}, h_{cd}, h_{sb})}{\text{maximize}} && \Phi_{SE}(P_D(h_{sd}, h_{cd}, h_{sb})) \\ & \text{subject to} && \text{C1: } \Phi_{EE}(P_D(h_{sd}, h_{cd}, h_{sb})) \geq \Gamma_{EE} \\ & && \text{C2: } P_D(h_{sd}, h_{cd}, h_{sb}) |h_{sb}|^2 \leq I_{th} \\ & && \text{C3: } P_D(h_{sd}, h_{cd}, h_{sb}) \leq P_{max} \\ & && \text{C4: } P_D(h_{sd}, h_{cd}, h_{sb}) \geq 0 \end{aligned} \quad (10)$$

where C1 reflects the minimum EE requirement ( $\Gamma_{EE} \geq 0$ ), C2 is related to interference constraint imposed by cellular communications, C3 means the maximum permitted transmission power constraint, and C4 ensures the transmission power is positive.

Since the threshold  $\Gamma_{EE}$  and the denominator of  $\Phi_{EE}$  is positive, constraint C4 can be guaranteed if the solution can satisfy the constraint C1. Moreover, for each specific transmission slot,  $h_{sb}$  remains unchanged and the interference received at the BS is determined by the transmission power. Thus, constraints C2 and C3 can be equalized to C5:  $P_D \leq P'_{max}$ , where  $P'_{max} = \min(P_{max}, I_{th} / |h_{sb}|^2)$ . We express the optimization problem in (10) equivalently as

$$\begin{aligned} & \underset{P_D(h_{sd}, h_{cd}, h_{sb})}{\text{maximize}} && \Phi_{SE}(P_D(h_{sd}, h_{cd}, h_{sb})) \\ & \text{subject to} && \text{C1, C5.} \end{aligned} \quad (11)$$

1) *Power Allocation Without Maximum Power Constraint:* In the following, we first settle the optimization problem without the transmission power constraint, i.e.,

$$\begin{aligned} & \underset{P_D(h_{sd}, h_{cd})}{\text{maximize}} && \Phi_{SE}(P_D(h_{sd}, h_{cd})) \\ & \text{subject to} && \text{C1.} \end{aligned} \quad (12)$$

*Theorem 1: The Karush-Kuhn-Tucker (KKT) conditions are both sufficient and necessary for the optimality of (12).*

*Proof:* The proof is presented in Appendix A. ■

Hence, denoting  $\ell \geq 0$  as the Lagrange multiplier, the Lagrangian associated with the problem (12) is given by

$$L(P_D(h_{sd}, h_{cd}), \ell) = \log_2 \left( 1 + \frac{P_D(h_{sd}, h_{cd}) |h_{sd}|^2}{N_0 + P_C |h_{cd}|^2} \right) + \ell \left( \log_2 \left( 1 + \frac{P_D(h_{sd}, h_{cd}) |h_{sd}|^2}{N_0 + P_C |h_{cd}|^2} \right) - \Gamma_{EE} (\varepsilon P_D(h_{sd}, h_{cd}) + P_0) \right) \quad (13)$$

The solution for the optimal power should satisfy

$$\frac{\partial L(P_D(h_{sd}, h_{cd}), \ell)}{\partial P_D(h_{sd}, h_{cd})} = \frac{(1 + \ell) A}{\ln 2 (1 + A P_D(h_{sd}, h_{cd})) - \varepsilon \ell \Gamma_{EE}} = 0 \quad (14)$$

where  $A = \frac{|h_{sd}|^2}{N_0 + P_C |h_{cd}|^2}$ . From (14), we have

$$P_D(h_{sd}, h_{cd}) = \frac{1 + \ell}{\ln 2 \varepsilon \ell \Gamma_{EE}} - \frac{1}{A}. \quad (15)$$

According to KKT conditions, if C1 is satisfied with strict inequality, the parameter  $\ell$  must be zero. Otherwise, the value of  $\ell$  can be obtained by substituting (15) into C1 and setting the inequality to equality, i.e.,

$$\log_2 \left( \frac{(1 + \ell) A}{\ln 2 \varepsilon \ell \Gamma_{EE}} \right) - \Gamma_{EE} \left( \varepsilon \frac{1}{A} \left( \frac{(1 + \ell) A}{\ln 2 \varepsilon \ell \Gamma_{EE}} - 1 \right) + P_0 \right) = 0. \quad (16)$$

We can get the optimal value  $\ell^*$  numerically through root-finding search algorithm. Considering that the transmit power is nonnegative, the optimal transmission power  $P_D(h_{sd}, h_{cd})$  is given by

$$P'_D(h_{sd}, h_{cd}) = \left( \frac{1 + \ell^*}{\ln 2 \varepsilon \ell^* \Gamma_{EE}} - \frac{1}{A} \right)^+ \quad (17)$$

where  $(x)^+$  means  $\max(0, x)$ .

2) *Power Allocation With Maximum Power Constraint:* In this part, we focus on discussing the problem taking the constraint C5 into account. In this case, utilizing the results obtained above, the solution for the optimal problem can be divided into two regions.

(1)  $P'_D(h_{sd}, h_{cd}) \geq P'_{\max}$ : In this case, if the obtained optimal power destroys the constraint on the maximum transmission power, it would be invalid for practical system application. As is known, SE function is a monotone increasing function in transmission power. As a consequence, the optimal problem with both EE and transmission power constrains can be simplified into a power constrained SE maximization problem. If  $\Phi_{EE}(P'_{\max}) \leq \Gamma_{EE}$ , there is no feasible solution for (10) for the transmit power is too small to achieve the minimum EE. If  $\Phi_{EE}(P'_{\max}) \geq \Gamma_{EE}$ ,  $P_D^*(h_{sd}, h_{cd}) = P'_{\max}$ .

(2)  $P'_D(h_{sd}, h_{cd}) \leq P'_{\max}$ : In this case, the extra transmission power constraint does not affect the optimal solution. The optimal power of (11) is the same as (12), i.e.,  $P_D^*(h_{sd}, h_{cd}, h_{sb}) = P'_D$ .

In summary, the optimal transmission power of (10) can be expressed as

$$P_D^*(h_{sd}, h_{cd}, h_{sb}) = \begin{cases} 0 & \text{if } \Phi_{EE}(P_D) < \Gamma_{EE} \\ \min \left( \left( v \frac{1 + \ell}{\ln 2 \varepsilon \ell \Gamma_{EE}} - \frac{1}{A} \right)^+, P'_{\max} \right) & \text{else} \end{cases} \quad (18)$$

### C. Power Allocation in Low VTD Scenarios

In this subsection, we concentrate on the EE and SE trade-off in low VTD scenarios. Specifically, the optimal power allocation strategy is formulated as an optimization problem with the objective of maximizing EE subject to the minimum SE requirement and the interference constraint. By denoting  $\Gamma_{SE}$  as the SE threshold, the optimization problem can be formulated as

$$\begin{aligned} & \underset{P_D(h_{sd}, h_{cd}, h_{sb})}{\text{maximize}} && \Phi_{EE}(P_D(h_{sd}, h_{cd}, h_{sb})) \\ & \text{subject to} && \text{C2, C3, C4} \\ & && \text{C6: } \Phi_{SE}(P_D(h_{sd}, h_{cd}, h_{sb})) \geq \Gamma_{SE}. \end{aligned} \quad (19)$$

The constraint C6 imposed in (19) represents the minimum SE requirement ( $\Gamma_{SE} \geq 0$ ). Similarly, the constraints C2 and C3 are equivalent to the C5:  $P_D(h_{sd}, h_{cd}, h_{sb}) \leq P'_{\max}$ . Then, we have the following equivalent optimization problem

$$\begin{aligned} & \underset{P_D(h_{sd}, h_{cd}, h_{sb})}{\text{maximize}} && \Phi_{SE}(P_D(h_{sd}, h_{cd}, h_{sb})) \\ & \text{subject to} && \text{C5, C6.} \end{aligned} \quad (20)$$

1) *Power allocation without maximum power constraint:* Firstly, we settle the optimization problem without the transmission power constraint, i.e.,

$$\begin{aligned} & \underset{P_D(h_{sd}, h_{cd})}{\text{maximize}} && \Phi_{EE}(P_D(h_{sd}, h_{cd})) \\ & \text{subject to} && \text{C6.} \end{aligned} \quad (21)$$

The expression of  $\Phi_{EE}$  in (7) can be rewritten as

$$\begin{aligned} \Phi_{EE}(P_D(h_{sd}, h_{cd})) &= \frac{f(P_D(h_{sd}, h_{cd}))}{g(P_D(h_{sd}, h_{cd}))} \\ &= \frac{\log_2 \left( 1 + \frac{P_D(h_{sd}, h_{cd}) |h_{sd}|^2}{N_0 + P_C |h_{cd}|^2} \right)}{\varepsilon P_D(h_{sd}, h_{cd}) + P_0}. \end{aligned} \quad (22)$$

According to Charnes-Cooper transform [36], we apply suitable variable transformation to reformulate the optimization problem to an equivalent problem. By applying the transformation  $x = \frac{P_D(h_{sd}, h_{cd})}{g(P_D(h_{sd}, h_{cd}))}$  and  $k = \frac{1}{g(P_D(h_{sd}, h_{cd}))}$ , we have

$$\begin{aligned} & \text{maximize} && kf \left( \frac{x}{k} \right) \\ & \text{subject to} && k \left( \Gamma_{SE} - \Phi_{SE} \left( \frac{x}{k} \right) \right) \leq 0 \\ & && kg \left( \frac{x}{k} \right) = 1 \end{aligned} \quad (23)$$

in which the equality constraint is not necessarily convex. To obtain the closed-form expression of optimal power, we utilize a relaxed problem according to Theorem 2.

*Theorem 2:* Since  $f(P_D(h_{sd}, h_{cd})) > 0$ , the problem in (23) is equivalent to the problem in (24).

$$\begin{aligned} & \text{maximize } kf\left(\frac{x}{k}\right) \\ & \text{subject to } k\left(\Gamma_{SE} - \Phi_{SE}\left(\frac{x}{k}\right)\right) \leq 0 \\ & \quad kg\left(\frac{x}{k}\right) \leq 1. \end{aligned} \quad (24)$$

*Proof:* The proof is presented in Appendix B. ■

According to [37], the objective function in (24) is a convex program in  $P_D$ , thus the KKT conditions are both sufficient and necessary for the optimality of (24). Hence, refer to  $P_D = x/k$ , the Lagrangian associated with the problem (24) can be given by

$$\begin{aligned} & L(P_D(h_{sd}, h_{cd}), k, \mu, \nu) \\ & = \nu k \left( \Gamma_{SE} - \log_2 \left( 1 + \frac{P_D(h_{sd}, h_{cd}) |h_{sd}|^2}{N_0 + P_C |h_{cd}|^2} \right) \right) \\ & \quad + k \log_2 \left( 1 + \frac{P_D(h_{sd}, h_{cd}) |h_{sd}|^2}{N_0 + P_C |h_{cd}|^2} \right) \\ & \quad + \mu (k(\varepsilon P_D(h_{sd}, h_{cd}) + P_0) - 1) \end{aligned} \quad (25)$$

where  $\mu, \nu \geq 0$  are the Lagrange multipliers.

At the optimal point, we have

$$\frac{\partial L(P_D(h_{sd}, h_{cd}), k, \mu, \nu)}{\partial P_D(h_{sd}, h_{cd})} = \frac{kA(1-\nu)}{\ln 2(1+AP_D(h_{sd}, h_{cd})) + k\mu\varepsilon} = 0 \quad (26)$$

$$\begin{aligned} \frac{\partial L(P_D(h_{sd}, h_{cd}), k, \mu, \nu)}{\partial k} & = \log_2(1+AP_D(h_{sd}, h_{cd})) (1-\nu) \\ & \quad + \mu(\varepsilon P_D(h_{sd}, h_{cd}) + P_0) \\ & \quad + \nu \Gamma_{SE} = 0 \end{aligned} \quad (27)$$

$$\begin{aligned} \frac{\partial L(P_D(h_{sd}, h_{cd}), k, \mu, \nu)}{\partial \nu} & = k(\Gamma_{SE} - \log_2(1+AP_D(h_{sd}, h_{cd}))) = 0. \end{aligned} \quad (28)$$

From (26), we can obtain

$$P'_D(h_{sd}, h_{cd}) = \frac{\nu - 1}{\ln 2\varepsilon\mu} - \frac{1}{A}. \quad (29)$$

From (27) we have

$$\mu = \frac{(\nu - 1)\log_2(1+AP_D(h_{sd}, h_{cd})) - \nu\Gamma_{SE}}{\varepsilon P_D(h_{sd}, h_{cd}) + P_0}. \quad (30)$$

According to (27) and refer to that  $k > 0$ , at the optimal point we have

$$\Gamma_{SE} - \log_2(1+AP'_D(h_{sd}, h_{cd})) = 0. \quad (31)$$

By substituting (30) into (29), we obtain  $P_D(\nu)$  where  $P_D$  is expressed as a function of  $\nu$ . After substituting  $P_D(\nu)$  into (31), we can get an equation with respect to  $\nu$ , from which we can get the optimal value  $\nu^*$  numerically through root-finding search. Subsequently, we can get the optimal power of problem (21) by substituting  $\nu^*$  into  $P_D(\nu)$ , i.e.,  $P'_D = P_D(\nu^*)$ .

2) *Power allocation with maximum power constraint:* In this part, we focus on discussing the problem taking the constraint C5 into account. Following the similar discussion in high VTD scenarios, the optimal transmission power of (19) can be expressed as

$$P_D^*(h_{sd}, h_{cd}, h_{sb}) = \begin{cases} 0, & \text{if } \Phi_{SE}(P'_{\max}) < \Gamma_{SE} \\ \min\left(\left(\frac{\nu-1}{\ln 2\varepsilon\mu} - \frac{1}{A}\right)^+, P'_{\max}\right), & \text{else} \end{cases} \quad (32)$$

#### IV. ECONOMIC EFFICIENCY: A GENERAL EVALUATION CRITERION

In previous sections, we have investigated the EE-SE trade-off by formulating different optimization problems for high VTD and low VTD scenarios, respectively. Meanwhile, we also have obtained the optimal solutions expressed as functions of EE or SE threshold. It is worth noting that the EE/SE threshold plays a decisive role in system performance optimization. Whereas, how to determine the decisive parameters in EE-SE trade-off, i.e., SE and EE thresholds, should be further studied to facilitate the practicality of EE and SE trade-off. Motivated by [34] and [35], we employ the ECE as a complementary measure for EE and SE performance metrics. The ECE can provide a quantitative evaluation for the efficacy of trade-off from the perspective of benefit and cost of the whole system. Moreover, ECE can serve as a general metric, being applicable to scenario-related power allocation schemes proposed in this paper.

The ECE (in monetary unit per second) measures the profitability of the system and equals to the revenue minus the actual cost of provided services. It takes into account the capacity and power consumption, and therefore is a good performance metric that sufficiently characterizes the EE and SE [34]. We denote  $k_r$  and  $k_c$  as the revenue per bit and energy cost per Joule, respectively, both of which are measured in the same monetary. We denote  $R^{\text{ref}}$  as the referenced data rate and  $C_0$  as other costs (in monetary unit per second). Here,  $R^{\text{ref}}$  refers to the essential service expected by mobile D2D user. In this paper, the definition of ECE can be given as

$$\begin{aligned} \Phi_{\text{ECE}} & = k_r R^{\text{ref}} \log_2 \left( 1 + \frac{W}{R^{\text{ref}}} \log_2 \left( 1 + \frac{P_D^*(\Gamma_i) |h_{sd}|^2}{N_0 + P_C |h_{cd}|^2} \right) \right) \\ & \quad - (C_0 + k_c P^*(\Gamma_i)) \end{aligned} \quad (33)$$

where  $P^*(\Gamma_i) = \varepsilon P_D^*(\Gamma_i) + P_0$  and  $i \triangleq \{\text{EE}, \text{SE}\}$ . Specifically,  $\Gamma_{\text{EE}}$  represents the EE threshold in high VTD scenarios and  $\Gamma_{\text{SE}}$  represents SE threshold in low VTD scenarios, respectively. The first term and the second term on the right-hand side of (33) represent the revenue attainable and the corresponding operational cost, respectively. According to the observation in [35], a user is only willing to pay an extra premium on top of the basic service for a multiplicative increase in the attainable data rate. Thus, the attainable revenue grows incrementally with every new service rather than following the multiplicative growth in data rate. This economic trend is known as the law of diminishing returns and this leads to a logarithmic relationship between the attainable revenue and attainable data rate.

TABLE II  
CHANNEL PARAMETERS OF THE 3D V2V CHANNEL MODEL [30]

Scenarios	$K$	$\eta_{SB_1}$	$\eta_{SB_2}$	$\eta_{SB_3}$	$\eta_{DB}$	$k^1$	$k^2$	$k^3$
Low VTD	3.786	0.335	0.203	0.411	0.051	9.6	3.6	11.6
High VTD	0.156	0.126	0.126	0.063	0.685	0.6	1.3	11.6

Since the optimal transmit power obtained is an expression of  $\Gamma_{EE}$  or  $\Gamma_{SE}$ , the cost and the revenue are related to  $\Gamma_{EE}$  or  $\Gamma_{SE}$ , the value of which plays a decisive role in the efficacy of trade-off. Therefore, further optimization is required to determine the optimal values of  $\Gamma_{EE}$  or  $\Gamma_{SE}$ . To optimize the system performance from the perspective of benefits and costs, we formulate a generalized optimization problem maximizing the ECE in both high VTD and low VTD scenarios, i.e.,

$$\begin{aligned} & \underset{\Gamma_i}{\text{maximize}} \quad \Phi_{ECE} \\ & \text{subject to} \quad \Gamma_i \geq 0. \end{aligned} \quad (34)$$

As we are interested in investigating the interplay of these metrics rather than implementing an actual optimization algorithm in real time, we perform an exhaustive search for the optimal value of the EE/SE threshold. Here, the exhaustive search is conducted through ergodic search within the feasible region. It is worth noting that the EE/SE threshold is only an intermediate variable to obtain the optimal transmit power, which is the objective of this work. To this end, substituting the optimal threshold into the expression of optimal transmit power, i.e., Eq. (18) or Eq. (32), we can finally obtain the value of the optimal transmit power.

## V. RESULTS AND ANALYSIS

In this section, we evaluate the schemes described in previous sections through Monte Carlo simulations. In the simulations, the pathloss model between BS and users is  $PL = 128.1 + 37.6 \log_{10}(d \text{ [in Km]})$  and the pathloss model between users is  $PL = 148.1 + 40 \log_{10}(d \text{ [in Km]})$  [11]. Specific values of channel parameters of the 3D V2V channel model are given in Table II [30]. In the simulations, channel coefficients are generated by the sum-of-sinusoids simulation model proposed in [30] with  $N_1 = N_2 = N_3 = 40$ . We set  $N_0 = -174$  dBm/Hz and  $W = 1$  MHz. Unless specifically stated, we set  $d_{sd} = 300$  m,  $d_{cd} = 400$  m, and  $d_{sb} = 400$  m. For simplicity, we assume that the SU and the RU move toward each other and in the same speed  $v$ . Unless specifically stated, the velocity of the CU, i.e.,  $v_c$ , is set to zero. Unless specifically stated, we set  $k_r = k_r^0 = 1.55 \times 10^{-7}$  pence/bit,  $k_c = k_c^0 = 4.22 \times 10^{-5}$  pence/Joule,  $R^{\text{ref}} = 1$  kbps, and  $C_0 = 4.15 \times 10^{-4}$  pence/s [34], [35].

We firstly conduct numerical simulations to demonstrate the impact of  $P_0$  on the EE of underlying mobile D2D communications in both low and high VTD scenarios, as shown in Fig. 2. As expected, the larger the  $P_0$  is, the smaller the EE becomes. For each  $P_0$ , the EE increases in the beginning and deteriorates afterwards as  $P_D$  increases along  $\Phi_{SE}$ . Moreover, the EE in low VTD outperforms that in high VTD, where the signals suffer from poor propagation environment. Besides, for

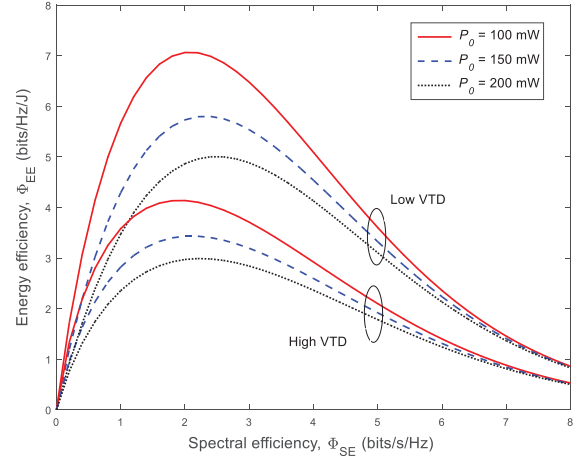


Fig. 2. EE versus SE with different  $P_0$  in low and high VTD scenarios ( $P_C = 23$  dBm,  $I_{th} = -70$  dBm, and  $v = 5$  m/s).

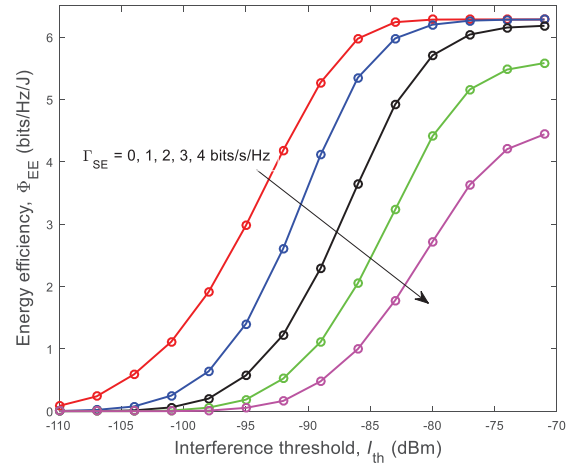


Fig. 3. EE versus interference threshold in a low VTD scenario ( $P_C = 23$  dBm,  $P_{\max} = 30$  dBm,  $P_0 = 100$  mW, and  $v = 5$  m/s).

different  $P_0$ , the curves in low VTD have a sharper head than in high VTD, implying that the discussion in section I is valid for different kinds of mobile equipment.

Fig. 3 depicts the EE of D2D communications versus the interference threshold with various spectral requirements in a low VTD scenario, where EE is maximized while guaranteeing the SE requirement by utilizing the power allocation scheme in (9). It can be observed that as  $I_{th}$  becomes larger, the EE of D2D communications increase in the beginning and tends to saturated eventually. This is because that the interference constraint is valid in the beginning and as it becomes looser, the maximum transmission power constrain begins to dominate. Moreover, the higher the spectral efficiency requirement is, i.e.,  $\Gamma_{SE}$  gets larger, the lower the EE is. This is because that  $\Phi_{EE}$  is the maximum achievable EE on feasible region  $(P_{\min}, P_{\max})$ . Here,  $P_{\min}$  is minimum required transmit power determined by the SE threshold and  $P_{\max}$  is the maximum permitted transmit power bounded by the interference constraint  $I_{th}$ . For a given  $I_{th}$ , as  $\Gamma_{SE}$  increases, the probability that  $P_{\min} > P_{\max}$  increases. When the feasible region is empty,  $\Phi_{EE}$  is zero. Therefore, from the

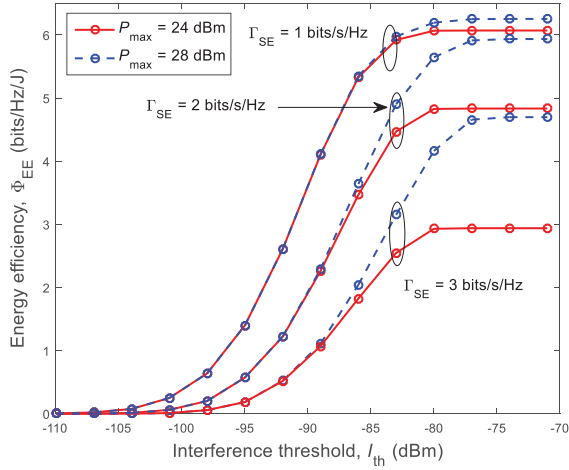


Fig. 4. EE with various SE requirement  $\Gamma_{SE}$  and maximum transmit powers  $P_{max}$  in a low VTD scenario ( $P_C = 23$  dBm,  $P_0 = 100$  mW, and  $v = 5$  m/s).

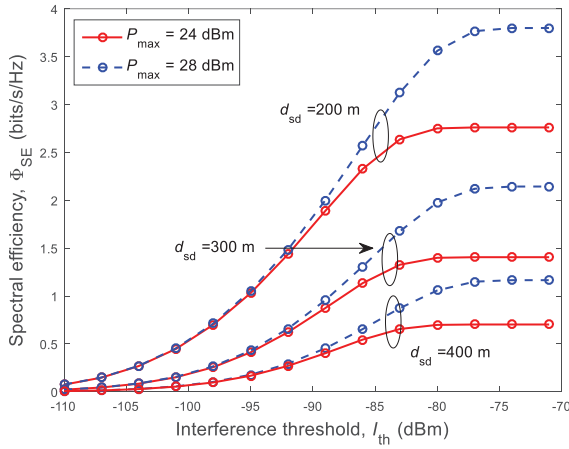


Fig. 5. SE versus interference threshold with different maximum transmit powers in a high VTD scenario ( $\Gamma_{EE} = 1$  bits/Hz/J,  $P_C = 23$  dBm,  $P_0 = 100$  mW, and  $v = 5$  m/s).

perspective of statistics, EE decreases with the SE requirement increases. This phenomenon indicates that for energy sensitive mobile users, the data rate should be restricted to achieve high EE when the bandwidth is fixed. In other words, in this case, never should we increase the transmission power to obtain high SE.

Fig. 4 shows the impact of the maximum transmission power  $P_{max}$  on the EE with different spectral requirements in a low VTD scenario. Being coincident with the conclusion obtained previously, the larger the  $P_{max}$  is or the smaller the  $\Gamma_{SE}$  is, the higher the EE we can obtain. It is interesting to note that as  $\Gamma_{SE}$  increases from 1 to 3, the EE gap between  $P_{max} = 24$  dBm and  $P_{max} = 28$  dBm gets larger, which implies that the effect the maximum transmission power becomes more pronounced.

We further study the performance in high VTD scenarios. We illustrate the SE versus interference threshold for different maximum transmission powers  $P_{max}$  and EE thresholds  $\Gamma_{EE}$  in Fig. 5 and Fig. 6, respectively. Similar to the observation made in low VTD, the SE increases with  $I_{th}$  in the beginning and tends to saturated eventually. For both figures, the longer the distance between D2D transmitter and receiver is, the lower

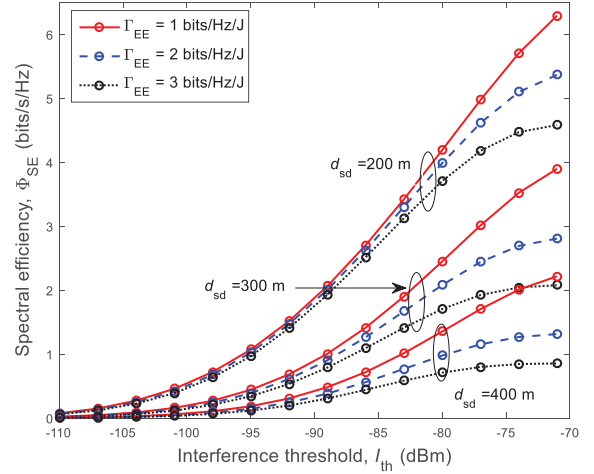


Fig. 6. SE versus interference threshold with different EE thresholds in a high VTD scenario ( $P_{max} = \infty$ ,  $P_C = 23$  dBm,  $P_0 = 100$  mW, and  $v = 5$  m/s).

the SE we can achieve. Note that both  $P_{max}$  and  $\Gamma_{EE}$  are related to the allowable transmission power. In Fig. 5, since the EE threshold  $\Gamma_{EE} = 1$  bits/Hz/J, which is relatively small compared with the maximum EE, the SE is mainly dominated by  $P_{max}$  and increases as  $P_{max}$  gets larger. While in Fig. 6 where we remove the maximum transmission power constraint, when  $\Gamma_{EE}$  gets larger, the feasible power region becomes smaller, which results in a lower SE.

In the following, we discuss the trade-off between EE and SE for both low and high VTD scenarios. In order to quantitatively illustrate the trade-off between EE and SE, we define  $\theta_{EE}$  and  $\theta_{SE}$  as the ratios of variation of EE and SE, respectively. According to the optimization problem in Section III, in low VTD scenarios, we have SE loss ratio  $\theta_{SE}^- = \frac{\Phi_{SE}^{max} - \Phi_{SE}^*}{\Phi_{SE}^{max}}$  and EE gain ratio  $\theta_{EE}^+ = \frac{\Phi_{EE}^* - \Phi_{EE}^{max}}{\Phi_{EE}^{max}}$ . Here,  $\Phi_{SE}^{max}$  is the maximum SE determined by  $P_{max}$  and  $I_{th}$ , and  $\Phi_{EE}^*$  is the corresponding EE. Moreover,  $\Phi_{EE}^{max}$  is the EE at the optimal power related to  $\Gamma_{SE}$ , and  $\Phi_{SE}^*$  is the corresponding SE. In high VTD scenarios, we define EE loss ratio  $\theta_{EE}^- = \frac{\Phi_{EE}^{max} - \Phi_{EE}^*}{\Phi_{EE}^{max}}$  and SE gain ratio  $\theta_{SE}^+ = \frac{\Phi_{SE}^* - \Phi_{SE}^{max}}{\Phi_{SE}^{max}}$ . Here,  $\Phi_{EE}^{max}$  is the maximum EE achieved within the feasible power region and  $\Phi_{SE}^{max}$  is the corresponding SE. Moreover,  $\Phi_{SE}^*$  is the SE at the optimal power related to  $\Gamma_{EE}$ , and  $\Phi_{EE}^*$  is the corresponding EE.

We present the EE gain ratio versus SE loss ratio with different  $\Phi_{SE}^{max}$  and  $P_0$  in Fig. 7. As expected, as SE loss ratio increases, the EE gain ratio keeps rising. The larger  $\Phi_{SE}^{max}$  is, more gains can be obtained for EE, which is resulted from the sharp slop of EE and SE trade-off curve in low VTD. Thus, it is meaningful to sacrifice SE for EE enhancement, especially when users are energy sensitive and require for high SE. Moreover, Fig. 8 shows the EE gain ratio with different velocities and distances between SU and DU, where the curve with longer communication distance or higher velocity has a greater slop. Furthermore, Fig. 9 illustrates the impact of interference threshold and interference power on the EE gain ratio. As observed, the tighter interference constraint is, i.e.,  $I_{th}$  is smaller, the larger  $\theta_{EE}^+$  is. This is because that according to the proposed power allocation

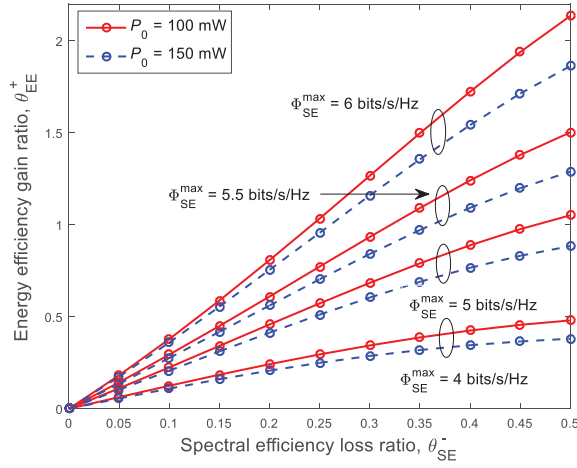


Fig. 7. EE gain ratio with different maximum SE in a low VTD scenario ( $P_C = 23$  dBm,  $P_{\max} = \infty$ ,  $I_{th} = -70$  dBm, and  $v = 5$  m/s).

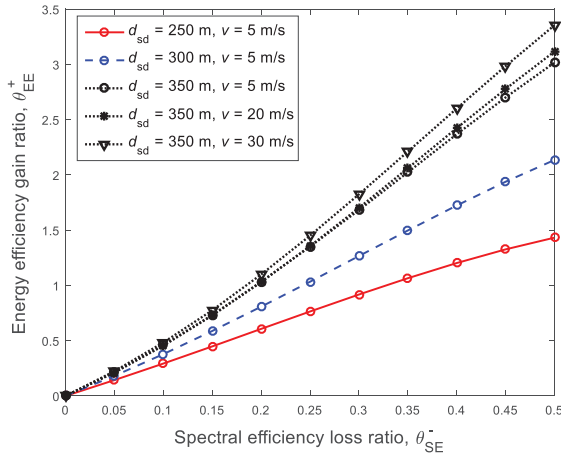


Fig. 8. EE gain ratio with different velocities and distances between S and D in a low VTD scenario ( $P_C = 23$  dBm,  $P_{\max} = \infty$ ,  $I_{th} = -70$  dBm,  $P_0 = 100$  mW, and  $\Phi_{SE}^{\max} = 6$  bps/Hz).

scheme, if the interference constraint becomes tight, users are rejected to communicate when they suffer from extremely poor channel conditions. From Fig. 7-Fig. 9, we can conclude that when D2D communications occurs in terrible communication environment, no matter suffering poor communication link condition or much interference from cellular communication, we can obtain significant gains in EE by reducing SE.

Next, we conduct simulation to study the SE gain in high VTD scenarios. Fig. 10 illustrates the SE gain ratio with different interference thresholds and power consumptions. It can be seen that different from the EE gain in low VTD scenarios, the SE gain increases as the interference constraint increase, i.e., the looser the  $I_{th}$  is. This phenomenon can be explained by integrating two facts into account. One is that the optimal EE is usually obtained with small transmission power as shown in Fig. 1, and another is the tight interference constraint restricts the maximum feasible transmission power, which leads to smaller achievable SE. Fig. 11 presents the SE gain ratio with different interference and communication distances. We can see that a rather little loss in EE from its maximum value, i.e.,  $\theta_{EE}^-$  is close to 0, generates a significant

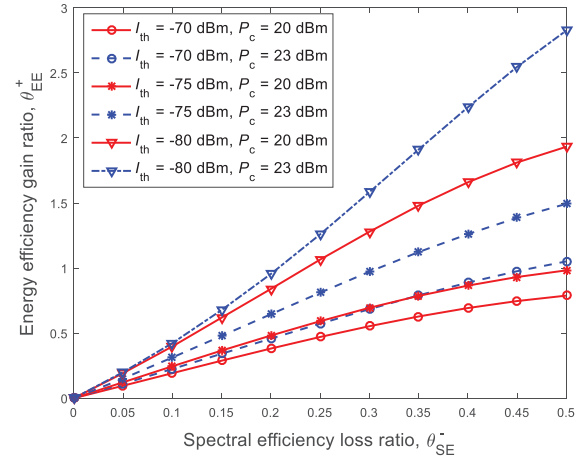


Fig. 9. EE gain ratio with different interference thresholds and cellular user transmit powers in a low VTD scenario ( $P_{\max} = \infty$ ,  $P_0 = 100$  mW,  $v = 5$  m/s, and  $\Phi_{SE}^{\max} = 5$  bps/Hz).

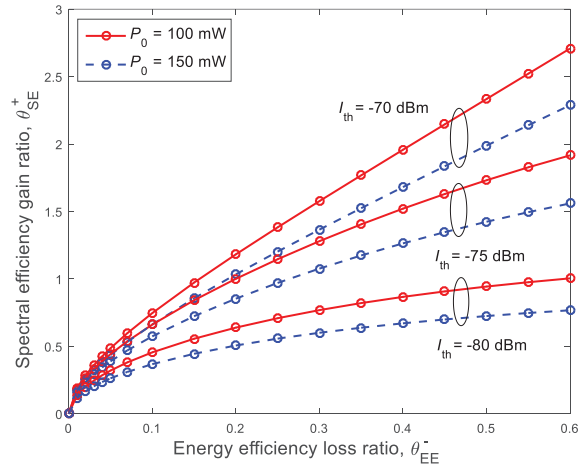


Fig. 10. SE gain ratio with different interference thresholds in a high VTD scenario ( $P_{\max} = \infty$  and  $v = 5$  m/s).

gain in SE. Moreover,  $\theta_{SE}^+$  increases with  $d_{sd}$  increases, which implies that when the communication distance is long, we tend to sacrifice EE since we can achieve great gains in SE.

We have illustrated EE gains and SE gains in low VTD and high VTD scenarios, which indicates that the more the EE (SE) derogation is, the larger the SE (EE) gain is. Whereas, the overall performance cannot be optimized relying on single performance metric, which indicates that we need to manage the trade-off between EE and SE, rather than sacrificing one of them blindly. To determine the decrement of either EE or SE, we exploit the ECE to evaluate the trade-off between EE and SE. Specifically, we show the economic efficiency  $\Phi_{ECE}$  versus the SE loss ratio  $\theta_{SE}^-$  and EE loss ratio  $\theta_{EE}^-$  in Fig. 12 and Fig. 13, respectively. Firstly, for each case, there exists an optimal value of  $\theta_{SE}^-$  or  $\theta_{EE}^-$  that maximizes  $\Phi_{ECE}$ , which is the corresponding optimal operating point of SE or EE. Moreover, for low VTD scenarios, when the communication distance or the velocity increases, the optimal value of  $\theta_{SE}^-$  maximizing ECE tends to move right, which indicates that in a worse communication condition, we prefer to give up more SE from the perspective

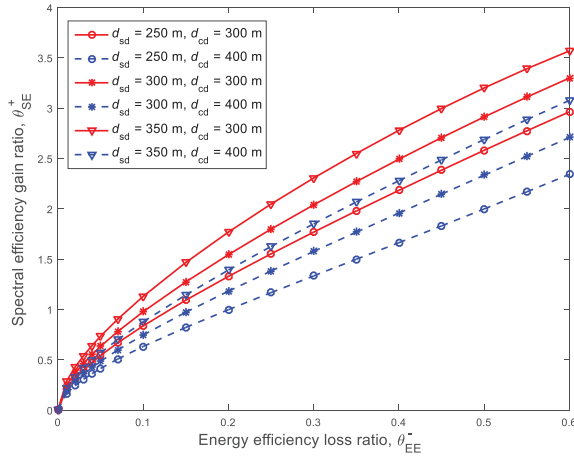


Fig. 11. SE gain ratio with different interference and communication distances in a high VTD scenario ( $P_0 = 100$  mW,  $I_{th} = -70$  dBm,  $P_{max} = \infty$ , and  $v = 5$  m/s).

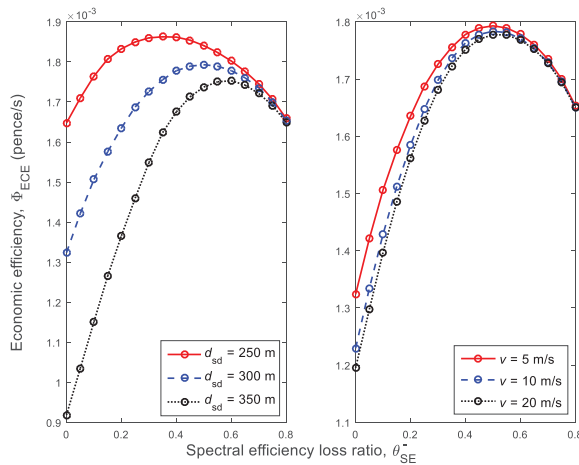


Fig. 12. ECE versus SE loss ratio in a low VTD scenario ( $P_0 = 100$  mW,  $I_{th} = -70$  dBm,  $P_{max} = \infty$ ,  $P_C = 23$  dBm,  $\Phi_{SE}^{max} = 6$  bps/Hz, and  $v = 5$  m/s).

of economic efficiency. However, for high VTD scenarios, when the communication distance decreases or the interference distance increases, the optimal value of  $\theta_{EE}^-$  maximizing ECE tends to move right, which indicates that in a better communication condition, we prefer to sacrifice more EE from the perspective of economic efficiency. Based on the above observations, we can conclude that ECE is a generalized metric valid for different scenarios and has the ability to capture the channel characteristics.

At last, we take high VTD scenarios as an example to reveal the impact of revenue and cost parameters on the ECE performance. Similar to the observation in Fig. 12 and Fig. 13, ECE increases in the beginning and decreases afterwards, existing an optimal  $\theta_{EE}^-$  that maximizes  $\Phi_{ECE}$ . As expected, larger revenue (larger  $k_T$ ) or smaller cost (smaller  $k_C$ ) results in higher  $\Phi_{ECE}$ . Moreover, the optimal point tends to move towards the high  $\theta_{EE}^-$  regime when either  $k_T$  gets larger, or  $k_C$  gets smaller. In other words, with large revenue per bit or small energy cost per Joule, we prefer to pursue SE to maximize the profit of communications service. As shown in Fig. 14,

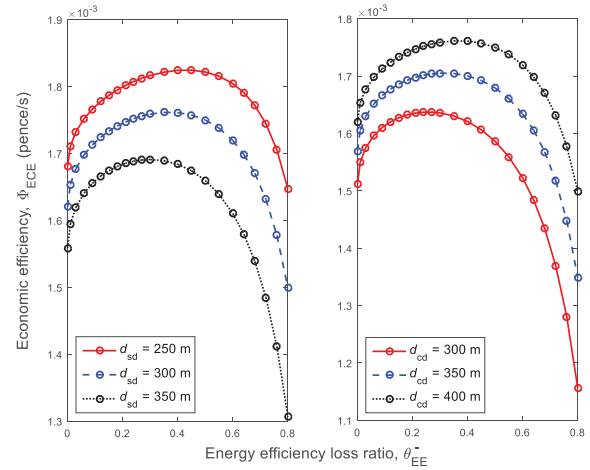


Fig. 13. ECE versus EE loss ratio in a high VTD scenario ( $P_0 = 150$  mW,  $I_{th} = -70$  dBm,  $P_{max} = \infty$ ,  $P_C = 23$  dBm, and  $v = 5$  m/s).

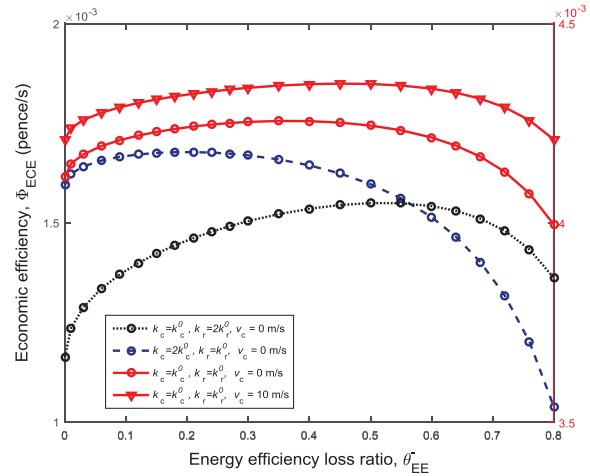


Fig. 14. ECE with different revenue and cost parameters in a high VTD scenario ( $P_0 = 150$  mW,  $I_{th} = -70$  dBm,  $P_{max} = \infty$ ,  $P_C = 23$  dBm, and  $v = 5$  m/s).

when the velocity of the CU increases from 0 m/s to 10 m/s, the system can achieve higher ECE. Larger velocity of the CU results in faster fading and then poorer interfering link quality, from which mobile D2D communications benefit. In addition, the optimal value of  $\theta_{SE}^-$  moves right, indicating that in a better communication condition, we can sacrifice more EE to maximize the system profit.

## VI. CONCLUSIONS

In this paper, we have proposed two different power allocation schemes and investigated the EE-SE trade-off for underlying mobile D2D communications, where a 3D V2V channel model has been adopted to characterize the impact of vehicular environments on both EE and SE. Considering that VTD significantly affects the performance of EE and SE, we have proposed to maximize SE subject to EE requirement in high VTD scenarios and maximize EE subject to SE in low VTD scenarios. Based on obtained optimal powers expressed as functions of SE or EE threshold, ECE has been employed as a general criterion to assess the efficacy of trade-off in different VTD scenarios. Simulation results have shown that ECE can

serve as a generalized metric for EE-SE trade-off in vehicular environment under different communication conditions.

#### APPENDIX A PROOF OF THEOREM 1

The objective function is a logarithmic function with respect to  $P_D$  and thus, it is concave according to [37]. As the objective function is differentiable, it is Pseudo-concavity in  $P_D$ . On the other hand, since the denominator of the constraint is affine, C1 is quasi-concave in  $P_D$ . Let  $\ell$  be the multiplier. The KKT conditions of (12) can be written as

$$\nabla\Phi_{SE}(P_D) + \ell_i\nabla C_i(P_D) = 0 \quad (35)$$

$$\ell_i C_i(P_D) = 0 \quad (36)$$

$$\ell_i \geq 0, C_i(P_D) \geq 0. \quad (37)$$

According to [37], under the constraint qualification assumption, the necessity of is a simple and standard result and it holds. Now we turn to the sufficiency proof part.

Let us assume that  $\tilde{P}_D$  is the optimal power allocation of (12) corresponding to the multiplier  $\tilde{\ell}_i$ . Let us assume that there exists another feasible  $\hat{P}_D$ . so that  $\Phi_{SE}(\hat{P}_D) > \Phi_{SE}(\tilde{P}_D)$ . Referring to the fact that the objective function is Pseudo-concavity in  $P_D$ , we have

$$\nabla\Phi_{SE}(\tilde{P}_D) \left( \hat{P}_D - \tilde{P}_D \right) > 0. \quad (38)$$

Now, we define  $I = \{i : \ell_i > 0\}$ . Then, the constraint  $C_i(P_D) = 0$ . As a result, for  $i \in I$ ,  $C_i(\hat{P}_D) \geq 0 = C_i(\tilde{P}_D)$  holds. Referring to the fact that the objective function is quasi-concavity in  $P_D$ , we have

$$\nabla C_i(\tilde{P}_D) \left( \hat{P}_D - \tilde{P}_D \right) > 0. \quad (39)$$

Let us assume that  $i \notin I$  and then  $\ell = 0$ . Hence, we obtain

$$\left( \nabla\Phi_{SE}(\tilde{P}_D) + \ell\nabla C_i(P_D) \right) \left( \hat{P}_D - \tilde{P}_D \right) > 0 \quad (40)$$

which contradicts (35). Thus, the assumption that there exists another feasible  $\hat{P}_D$  that is the optimal power allocation of (12) is not established and the sufficiency proof is completed.

#### APPENDIX B PROOF OF THEOREM 2

Since  $f(P_D) > 0$ , the problem in (24) is equivalent to the problem in (23). First, we denote  $P$ ,  $P_1$  and  $P_2$  as the feasible set of (21), (23), and (24). Then we have

$$P_1 = \left\{ x_1, k_1 \in R_{++} \times R_{++} : \frac{x_1}{k_1} \in P, k_1 g\left(\frac{x_1}{k_1}\right) = 1 \right\} \quad (41)$$

$$P_2 = \left\{ x_2, k_2 \in R_{++} \times R_{++} : \frac{x_2}{k_2} \in P, k_2 g\left(\frac{x_2}{k_2}\right) \leq 1 \right\} \quad (42)$$

where  $R_{++}$  is the set of positive real numbers. Obviously, we have  $P_1 \subseteq P_2$ . To complete the proof, we should prove that all elements in  $P_2 \setminus P_1$  are suboptimal for (24). For any  $(x_2, k_2) \in P_2$ , the following expression is satisfied:

$$k_2 g\left(\frac{x_2}{k_2}\right) = \sigma \in (0, 1]. \quad (43)$$

Then, we assume that  $x_1 = x_2/\sigma$  and  $k_1 = k_2/\sigma$ . Thus, for any  $(x_2, k_2) \in P_2$ , there exists  $(x_1, k_1) \in P_1$  and  $\sigma \in (0, 1]$  that satisfy  $(x_2, k_2) = (\sigma x_1, \sigma k_1)$ , where  $\sigma < 1$  if  $(x_2, k_2) \in P_2 \setminus P_1$ . Referring to the fact that the SE function is non-negative, then we get

$$k_2 f\left(\frac{x_2}{k_2}\right) = \sigma k_1 f\left(\frac{x_1}{k_1}\right) \leq k_1 f\left(\frac{x_1}{k_1}\right). \quad (44)$$

Here, if  $(x_2, k_2) \in P_2 \setminus P_1$ , the inequality is strict. Until now, all the elements in  $P_2 \setminus P_1$  are suboptimal for (24). This completes the proof of Theorem 2.

#### REFERENCES

- [1] G. Fodor *et al.*, "An overview of device-to-device communications technology components in METIS," *IEEE Access*, vol. 4, pp. 3288–3299, 2016.
- [2] N. Lee, X. Lin, J. G. Andrews, and R. W. Heath, Jr., "Power control for D2D underlaid cellular networks: Modeling, algorithms, and analysis," *IEEE J. Sel. Areas Commun.*, vol. 33, no. 1, pp. 1–13, Jan. 2015.
- [3] A. Asadi, Q. Wang, and V. Mancuso, "A survey on device-to-device communication in cellular networks," *IEEE Commun. Surveys Tuts.*, vol. 16, no. 4, pp. 1801–1819, 4th Quart., 2014.
- [4] C.-X. Wang *et al.*, "Cellular architecture and key technologies for 5G wireless communication networks," *IEEE Commun. Mag.*, vol. 52, no. 2, pp. 122–130, Feb. 2014.
- [5] D. Feng, L. Lu, Y. Yuan-Wu, G. Li, S. Li, and G. Feng, "Device-to-device communications in cellular networks," *IEEE Commun. Mag.*, vol. 52, no. 4, pp. 49–55, Apr. 2014.
- [6] H. Min, J. Lee, S. Park, and D. Hong, "Capacity enhancement using an interference limited area for device-to-device uplink underlaying cellular networks," *IEEE Trans. Wireless Commun.*, vol. 10, no. 12, pp. 3995–4000, Dec. 2011.
- [7] D. Feng, L. Lu, Y. Yuan-Wu, G. Y. Li, G. Feng, and S. Li, "Device-to-device communications underlaying cellular networks," *IEEE Trans. Commun.*, vol. 61, no. 8, pp. 3541–3551, Aug. 2013.
- [8] T. Kim and M. Dong, "An iterative Hungarian method to joint relay selection and resource allocation for D2D communications," *IEEE Wireless Commun. Lett.*, vol. 3, no. 6, pp. 625–628, Dec. 2014.
- [9] L. Xu, C. Jiang, Y. Shen, T. Q. S. Quek, Z. Han, and Y. Ren, "Energy efficient D2D communications: A perspective of mechanism design," *IEEE Trans. Wireless Commun.*, vol. 15, no. 11, pp. 7272–7285, Nov. 2016.
- [10] D. Wen, G. Yu, and L. Xu, "Energy-efficient mode selection and power control for device-to-device communications," in *Proc. IEEE WCNC*, Doha, Qatar, Apr. 2016, pp. 1–7.
- [11] R. Zhang, Y. Li, Y. Ruan, H. Zhang, W. Wang, and W. Wang, "CQI-based interference management scheme for D2D communication underlaying cellular networks," in *Proc. IEEE WCNCW*, New Orleans, LA, USA, Mar. 2015, pp. 347–351.
- [12] Y. Jiang, Q. Liu, F. Zheng, X. Gao, and X. You, "Energy-efficient joint resource allocation and power control for D2D communications," *IEEE Trans. Veh. Technol.*, vol. 65, no. 8, pp. 6119–6127, Aug. 2016.
- [13] T. D. Hoang, L. B. Le, and T. Le-Ngoc, "Energy-efficient resource allocation for D2D communications in cellular networks," in *Proc. IEEE ICC*, London, U.K., Jun. 2015, pp. 2943–2948.
- [14] J. Pérez-Romero, J. Sánchez-González, R. Agustí, B. Lorenzo, and S. Glisic, "Power-efficient resource allocation in a heterogeneous network with cellular and D2D capabilities," *IEEE Trans. Veh. Technol.*, vol. 65, no. 11, pp. 9272–9286, Nov. 2016.
- [15] S. Xiao, X. Zhou, D. Feng, Y. Yuan-Wu, G. Y. Li, and W. Guo, "Energy-efficient mobile association in heterogeneous networks with device-to-device communications," *IEEE Trans. Wireless Commun.*, vol. 15, no. 8, pp. 5260–5271, Aug. 2016.
- [16] K. Yang, S. Martin, C. Xing, J. Wu, and R. Fan, "Energy-efficient power control for device-to-device communications," *IEEE J. Sel. Areas Commun.*, vol. 34, no. 12, pp. 3208–3220, Dec. 2016.
- [17] B. Badic, C. Drewes, I. Karls, and M. Mueck, *Rolling Out 5G: Use Cases, Applications, and Technology Solutions*. New York, NY, USA: Apress, 2016.
- [18] X. Cao, L. Liu, Y. Cheng, L. X. Cai, and C. Sun, "On optimal device-to-device resource allocation for minimizing end-to-end delay in VANETs," *IEEE Trans. Veh. Technol.*, vol. 65, no. 10, pp. 7905–7916, Oct. 2016.

- [19] N. Cheng *et al.*, "Performance analysis of vehicular device-to-device underlay communication," *IEEE Trans. Veh. Technol.*, vol. 66, no. 6, pp. 5409–5421, Jun. 2017.
- [20] Y. Ren, F. Liu, Z. Liu, C. Wang, and Y. Ji, "Power control in D2D-based vehicular communication networks," *IEEE Trans. Veh. Technol.*, vol. 64, no. 12, pp. 5547–5562, Dec. 2015.
- [21] W. Sun, E. G. Ström, F. Brännström, K. C. Sou, and Y. Sui, "Radio resource management for D2D-based V2V communication," *IEEE Trans. Veh. Technol.*, vol. 65, no. 8, pp. 6636–6650, Aug. 2016.
- [22] W. Sun, D. Yuan, E. Ström, and F. Brännström, "Cluster-based radio resource management for D2D-supported safety-critical V2X communications," *IEEE Trans. Wireless Commun.*, vol. 15, no. 4, pp. 2756–2769, Apr. 2016.
- [23] M. Botsov, M. Klügel, W. Kellerer, and P. Fertl, "Location-based resource allocation for mobile D2D communications in multicell deployments," in *Proc. IEEE ICCW*, London, U.K., Jun. 2015, pp. 2444–2450.
- [24] M. Boban, T. T. V. Vinhoza, M. Ferreira, J. Barros, and O. K. Tonguz, "Impact of vehicles as obstacles in vehicular ad hoc networks," *IEEE J. Sel. Areas Commun.*, vol. 29, no. 1, pp. 15–28, Jan. 2011.
- [25] X. Cheng, L. Yang, and X. Shen, "D2D for intelligent transportation systems: A feasibility study," *IEEE Trans. Intell. Trans. Syst.*, vol. 16, no. 4, pp. 1784–1793, Jan. 2015.
- [26] A. Paier *et al.*, "Non-WSSUS vehicular channel characterization in highway and urban scenarios at 5.2 GHz using the local scattering function," in *Proc. IEEE WSA*, Vienna, Austria, Feb. 2008, pp. 9–15.
- [27] X. Ge, J. Chen, C.-X. Wang, J. Thompson, and J. Zhang, "5G green cellular networks considering power allocation schemes," *Sci. China Inf. Sci.*, vol. 59, no. 2, pp. 1–14, Feb. 2016.
- [28] Z. Zhou, M. Dong, K. Ota, J. Wu, and T. Sato, "Energy efficiency and spectral efficiency tradeoff in device-to-device (D2D) communications," *IEEE Wireless Commun. Lett.*, vol. 3, no. 5, pp. 485–488, Oct. 2014.
- [29] F. Haider, C. X. Wang, H. Haas, E. Hepsaydir, X. Ge, and D. Yuan, "Spectral and energy efficiency analysis for cognitive radio networks," *IEEE Trans. Wireless Commun.*, vol. 14, no. 6, pp. 2969–2980, Jun. 2015.
- [30] Y. Yuan, C.-X. Wang, X. Cheng, B. Ai, and D. I. Laurenson, "Novel 3D geometry-based stochastic models for non-isotropic MIMO vehicle-to-vehicle channels," *IEEE Trans. Wireless Commun.*, vol. 13, no. 1, pp. 298–309, Jan. 2014.
- [31] K. P. Peppas, P. S. Bithas, G. P. Efthymoglou, and A. G. Kanatas, "Space shift keying transmission for intervehicular communications," *IEEE Trans. Intell. Transp. Syst.*, vol. 17, no. 12, pp. 3635–3640, Dec. 2016.
- [32] S. Beygi, U. Mitra, and E. G. Ström, "Nested sparse approximation: Structured estimation of V2V channels using geometry-based stochastic channel model," *IEEE Trans. Signal Process.*, vol. 63, no. 18, pp. 4940–4955, Sep. 2015.
- [33] S. Huang, H. Chen, J. Cai, and F. Zhao, "Energy efficiency and spectral-efficiency tradeoff in amplify-and-forward relay networks," *IEEE Trans. Veh. Technol.*, vol. 62, no. 9, pp. 4366–4378, Nov. 2013.
- [34] P. Patcharamaneepakorn *et al.*, "Spectral, energy, and economic efficiency of 5G multicell massive MIMO systems with generalized spatial modulation," *IEEE Trans. Veh. Technol.*, vol. 65, no. 12, pp. 9715–9731, Dec. 2016.
- [35] I. Ku, C.-X. Wang, and J. S. Thompson, "Spectral, energy and economic efficiency of relay-aided cellular networks," *IET Commun.*, vol. 7, no. 14, pp. 1476–1486, 2013.
- [36] A. Charnes and W. W. Cooper, "Programming with linear fractional functionals," *Naval Res. Logistics Quart.*, vol. 9, nos. 3–4, pp. 181–186, 1962.
- [37] S. Boyd and L. Vandenberghe, *Convex Optimization*. Cambridge, U.K.: Cambridge Univ. Press, 2004.



**Rui Zhang** received the B.S. and M.S. degrees in telecommunications engineering from Xidian University, Xi'an, China, in 2012 and 2015, respectively, where he is currently pursuing the Ph.D. degree in communication and information system. He was a Visiting Ph.D. Student under the supervision of Prof. C.-X. Wang with Heriot-Watt University, Edinburgh, U.K., from 2016 to 2017. His current research interests focus on device-to-device communications, vehicle-to-vehicle communications, radio resource allocation techniques, and energy efficient wireless networks.



**Yongzhao Li** (M'04–SM'17) received the B.S., M.S., and Ph.D. degrees in electronic engineering from Xidian University, Xi'an, China, in 1996, 2001, and 2005, respectively. In 1996, he joined Xidian University, where he is currently a Full Professor with the State Key Laboratory of Integrated Services Networks. As a Research Professor, he was with the University of Delaware, Newark, DE, USA, from 2007 to 2008, and the University of Bristol, Bristol, U.K., in 2011, respectively. He currently serves as the Vice Dean of the School of Telecommunications Engineering with Xidian University. He has published over 50 journal papers and 20 conference papers. His research interests include wideband wireless communications, signal processing for communications, and spatial communications networks. In 2008, he received the Best Paper Award at the IEEE ChinaCOM08 International Conference. Due to his excellent contributions in education and research, in 2012, he was awarded by the Program for New Century Excellent Talents in University, Ministry of Education, China.



**Cheng-Xiang Wang** (S'01–M'05–SM'08–F'17) received the B.Sc. and M.Eng. degrees in communication and information systems from Shandong University, China, in 1997 and 2000, respectively, and the Ph.D. degree in wireless communications from Aalborg University, Denmark, in 2004.

He was a Research Assistant with the Hamburg University of Technology, Hamburg, Germany, from 2000 to 2001, a Research Fellow at the University of Agder, Grimstad, Norway, from 2001 to 2005, and a Visiting Researcher with Siemens AG-Mobile Phones, Munich, Germany, in 2004. He has been with Heriot-Watt University, Edinburgh, U.K., since 2005, and became a Professor in wireless communications in 2011. He is also an Honorary Fellow at The University of Edinburgh, U.K., a Chair Professor of Shandong University, and a Guest Professor with Southeast University, China. He has co-authored two books, one book chapter, and over 320 papers in refereed journals and conference proceedings. His current research interests include wireless channel measurements/modeling and (B)5G wireless communication networks, including green communications, cognitive radio networks, high mobility communication networks, massive MIMO, millimeter wave communications, and visible-light communications.

Dr. Wang is a Fellow of the IET and HEA. He received nine Best Paper Awards from the IEEE GLOBECOM 2010, IEEE ICCT 2011, ITST 2012, IEEE VTC 2013-Spring, IWCMC 2015, IWCMC 2016, IEEE/CIC ICC 2016, and WPMC 2016. He has served as a Technical Program Committee (TPC) Member, the TPC Chair, and a General Chair for over 80 international conferences. He has served as an Editor for nine international journals, including the IEEE TRANSACTIONS ON WIRELESS COMMUNICATIONS from 2007 to 2009, the IEEE TRANSACTIONS ON VEHICULAR TECHNOLOGY since 2011, and the IEEE TRANSACTIONS ON COMMUNICATIONS since 2015. He was the Lead Guest Editor of the IEEE JOURNAL ON SELECTED AREAS IN COMMUNICATIONS Special Issue on Vehicular Communications and Networks. He was also a Guest Editor of the IEEE JOURNAL ON SELECTED AREAS IN COMMUNICATIONS Special Issue on Spectrum and Energy Efficient Design of Wireless Communication Networks and Special Issue on Airborne Communication Networks, and a Guest Editor of the IEEE TRANSACTIONS ON BIG DATA Special Issue on Wireless Big Data. He is recognized as a Web of Science 2017 Highly Cited Researcher.



**Yuhuan Ruan** received the B.S. degree in telecommunications engineering from Xidian University, Xi'an, China, in 2013, where she is currently pursuing the Ph.D. degree in communication and information system. She was a Visiting Ph.D. Student under the supervision of Prof. C.-X. Wang with Heriot-Watt University, Edinburgh, U.K., from 2016 to 2017. Her current research interests are in the fields of satellite-terrestrial networks, cooperative communications, cognitive radio techniques, and energy-efficient wireless networks.



**Yu Fu** received the B.Sc. degree in computer science from Huaqiao University, Fujian, China, in 2009, and the M.Sc. degree in information technology (mobile communications) and Ph.D. degree in wireless communications from Heriot-Watt University, Edinburgh, U.K., in 2010 and 2015, respectively.

He has been a Post-Doctoral Research Associate with Heriot-Watt University since 2015. His main research interests include advanced MIMO communication technologies, wireless channel modeling and simulation, RF tests, and software-defined networks.



**Hailin Zhang** (M'98) received the B.S. and M.S. degrees from Northwestern Polytechnic University, Xi'an, China, in 1985 and 1988, respectively, and the Ph.D. degree from Xidian University, Xi'an, in 1991. Since 1991, he has been with Xidian University, where he is currently a Senior Professor and a Ph.D. Adviser with the School of Telecommunications Engineering. He is currently the Director of the Key Laboratory in Wireless Communications Sponsored by the China Ministry of Information Technology, a Key Member of the State Key Laboratory of

Integrated Services Networks, one of the State Government Specially Compensated Scientists and Engineers, a Field Leader in telecommunications and information systems at Xidian University, and the Associate Director for the National 111 Project. He has recently published 78 papers in telecommunications journals and proceedings. His current research interests include key transmission technologies and standards on broadband wireless communications for 4G, 5G, and next-generation broadband wireless access systems.